

UC Berkeley

Homogeneous Charge Compression Ignition

Title

Landfill Gas Fueled HCCI Demonstration System

Permalink

<https://escholarship.org/uc/item/0qp039sp>

Authors

Blizman, Brandon J.

Makel, Darby B.

Mack, John Hunter

et al.

Publication Date

2006-09-18

LANDFILL GAS FUELED HCCI DEMONSTRATION SYSTEM

Brandon J Blizman
Makel Engineering, Inc
1585 Marauder St,
Chico, CA 95973
(530)-895-2770

bblizman@makelengineering.com

Darby B. Makel
Makel Engineering, Inc
1585 Marauder St,
Chico, CA 95973
(530)-895-2770

dmakel@makelengineering.com

J. Hunter Mack
Department of Mechanical Engineering
University of California
Hesse Hall 50-B
Berkeley, CA 94720

hmack@me.berkeley.edu

Robert W. Dibble
Department of Mechanical Engineering
University of California
6159 Etcheverry Hall
Berkeley, CA 94720

dibble@me.berkeley.edu

ABSTRACT

This demonstration system is intended to meet the California Energy Commission's primary goal of improving California's electric energy cost/value by providing a low-cost high-efficiency distributed power generation engine that runs on landfill gas. The project team led by Makel Engineering, Inc. includes UC Berkeley, CSU Chico and the Butte County Public Works Department.

The team has developed a reliable, multi-cylinder Homogeneous Charge Compression Ignition (HCCI) engine by converting a Caterpillar 3116, 6.6 liter diesel engine to operate in HCCI mode. This engine utilizes a simple and robust thermal control system. Typically, HCCI engines are based on standard diesel engine designs with reduced complexity and cost based on the well known principles of engine dynamics. Coupled to an induction generator, this HCCI genset allows for simplified power grid connection.

Testing with this HCCI genset allowed for the development of a control system to maintain optimal the inlet temperature and equivalence ratio. A brake thermal efficiency of 35.0% was achieved while producing less than 10.0 ppm of NOx and 30 kW of electrical power. Less than 5.0 ppm of NOx was recorded with a slightly lower brake thermal

efficiency. Tests were conducted with both natural gas and simulated landfill gas as a fuel source. This demonstration system has shown that landfill gas fueled Homogeneous Charge Compression Ignition engine technology is a viable technology for distributed power generation.

INTRODUCTION

This demonstration is intended to meet the California Energy Commission's (CEC) primary goal of improving California's electric energy cost/value by providing a low-cost high-efficiency distributed power generation engine that utilizes landfill gas (LFG) as a fuel source. In addition, this demonstration enables improving the environmental and public health costs/risk of California's electricity generation by efficiently using LFG to generate electricity, while removing methane - a potent green house gas - from the environment.

The research team has successfully operated a modified diesel engine in HCCI mode using natural gas (NG) and simulated landfill gas (SLFG) as fuel. The team has progressed to testing of the HCCI genset using landfill gas supplied from a port on the landfill gas collection and control system (GCCS) at the Neal Road Landfill (NRL) Solid Waste Management Facility in Butte County California.

HCCI Technology

Relative to spark ignition (SI) engines, HCCI engines are more efficient, approaching the efficiency of a diesel engine. This improved efficiency results from three sources: the elimination of throttling losses, the use of high diesel-like compression ratios, and a shorter combustion duration (since it is not necessary for a flame to propagate across the cylinder). Relative to diesel engines, HCCI engines have substantially lower emissions of particulate matter (PM) and Nitric Oxides (NO_x) [1-3]. These low emissions are a result of the dilute homogeneous mixture and low combustion temperatures. Because flame propagation is not required, dilution levels can be much higher than the levels tolerated by either SI or diesel engines. Combustion is induced throughout the charge volume by compression heating due the piston motion, and it will occur in almost any fuel/air/exhaust-gas mixture once the 800 to 1100 K (depending on the type of fuel) ignition temperature is reached. Additionally, the combustion duration in HCCI engines is much shorter than in diesels since it is not limited by the rate of fuel/air mixing, giving HCCI engines an efficiency advantage. HCCI engines offer the potential to be lower cost than diesel engines since they would likely use lower-pressure fuel-injection equipment.

Engine tests conducted by UC Berkeley before the start of this project have demonstrated that HCCI engines can achieve high diesel-like efficiencies with ultra-low NO_x and PM emissions (*i.e.*, below levels requiring after treatment) [4-6]. These tests have also shown that under optimized conditions HCCI combustion can be very repeatable, resulting in smooth engine operation. In addition, HCCI combustion has been achieved with a wide range of fuels suggesting the possibility of fuel-flexible engines suitable for landfill gas applications.

Technical Performance

The anticipated performance parameters for this HCCI genset were based on previous research and operation of HCCI engines at UC Berkeley. Research efforts for this genset have been conducted utilizing both NG and SLFG as a fuel source. Ongoing research has used LFG as fuel. A maximum brake thermal efficiency (BTE) of 35.0% was achieved while producing less than 10.0 ppm of NO_x. Less than 5.0 ppm of NO_x was recorded with a slightly lower BTE. A brief summary of the HCCI genset performance using NG as fuel is listed in Table 1.

Table 1 - HCCI Genset Performance with Natural Gas

Target Parameter	Goals	Achieved	
Equivalence Ratio	< 0.40	0.34	0.38
NO _x Emissions (ppm)	< 5.0	~ 4.0	~9.5
Stability	+/- 10%	+/- 3.0%	+/- 3.0%
Brake Thermal Efficiency	>35%	~33 %	~35 %

The subsequent sections of this document illuminate the uniqueness of this HCCI genset as well as summarize the performance and emissions results.

NOMENCLATURE

Abbreviation	Term
A/F	Air to Fuel
ATA	Air to Air
ATM	Atmosphere
BTE	Brake Thermal Efficiency
CAT	Caterpillar
CO	Carbon Monoxide
CO ₂	Carbon Dioxide
E-STOP	Emergency stop
GC	Gas Chromatograph
HCCI	Homogeneous Charge Compression Ignition
HTO	Heat Transfer Oil
ICTC	Individual Cylinder Temperature Control
KGPH	Kilograms per hour
kW	Kilowatt
LFG	Landfill Gas
LTA	Liquid to Air
η	Eta (efficiency)
NG	Natural Gas
NO _x	Nitric Oxide/Nitrogen Dioxide
NRL	Neal Road Landfill
O ₂	Oxygen
Φ	Phi (Equivalence ratio)
PM	Particulate Matter
RPM	Revolution Per Minute
SI	Spark Ignition
SLFG	Simulated Landfill Gas
TDC	Top Dead Center
UHC	Unburned Hydrocarbon

HCCI GENSET

The HCCI genset has been developed as a stationary power generation system powered via a modified diesel engine operating in HCCI mode. The generator system will eventually operate on LFG, utilizing this otherwise flared off fuel resource for producing electrical power. For development purposes, the fuel line can use propane from a tank and NG from the PG&E line. Carbon dioxide can be added as a diluent to NG to simulate LFG composition. This generator system consists of the following components: a modified fixed displacement

reciprocating engine, an electric generator, thermal conditioning system for air-fuel (A/F) mixing, instrumentation and actuators, and an automated control system. These components are described in the following sections. The genset specifications are listed in Table 2.

The HCCI genset, shown in Figure 1, consists of a simplified stock CAT 3116 engine coupled to a generator. Modifications to the stock engine include: the addition of partitions to the intake manifold cover and the replacement of stock intake with an individual cylinder temperature control (ICTC) manifold. Appropriate generator housing was selected to couple directly to the SAE 14 bell housing of the engine.

Table 2 - HCCI Genset Specifications

Parameter	Specification
Cylinders	6 (In-line)
Compression Ratio	16.7 : 1
Displacement	6.6 L
Oil Sump Capacity	21 Quart
Cooling	Air-Liquid (DEAC)
Turbocharged	1.5 ATM
Engine RPM	1800 RPM
Maximum Output Power (electric)	35 kW
Generator	Induction 440 VAC, 3-phase, 60 Hz
Size	5.0' X 8.0' X 6.0'
Weight	2800 lb

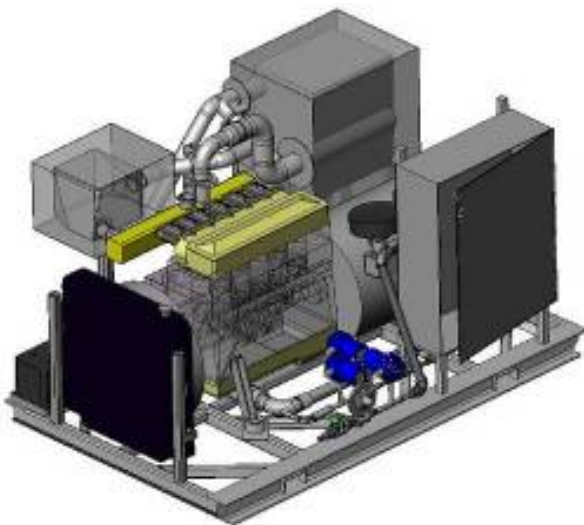


Figure 1 - 3D CAD Model of HCCI System-5.0 ft wide by 8.0 ft length by 6.0 ft height, weighing about 2800 lbs

INTAKE SYSTEM

In an HCCI engine, there is no spark plug and no fuel injector, and thus, no direct control of ignition timing. Combustion is accomplished by compression heating of the air-fuel charge in the cylinder to achieve auto-ignition. Ideally, this would occur when the cylinder is at top dead center (TDC). The primary control variable for sustaining operation in HCCI mode is the engine's intake temperature. To adjust the cylinder inlet temperature, a unique thermal conditioning system has been developed. It is comprised of intake ducts and valves, an air-to-air (ATA) heat exchanger, a liquid-to-air (LTA) heat exchanger, an ICTC manifold and heat transfer oil (HTO) reservoir.

Carbureted Intake LFG sample analyses from the Neal Road Landfill (NRL) indicate methane concentrations potentially as low as 30%. To accommodate lower methane concentrations, more total flow of landfill gas is fed to the HCCI genset. While operating with the lower methane content, is not viewed as a problem, a carbureted manifold, was added to the intake system to provide adequate air fuel mixing. An equivalence ratio (Φ) of about 0.30 is achieved while operating on NG. using carburetors with jets designed for propane operation at Φ of 1.0.

Thermal Conditioning System The thermal control of the LFG HCCI system is the primary means to control ignition timing of the engine. The system is designed with two heat exchanger systems to accommodate startup and steady state operation. The LTA heat exchanger coupled with a hot oil pump and reservoir allow for the proper intake temperature at startup to be reached. Once the engine is producing exhaust hot gases, the ATA heat exchanger provides the necessary heat input and the LTA heat exchanger is bypassed.

A heated 10-gallon reservoir allows for the pumping of heat transfer oil (HTO) through the LTA heat exchanger. Initially, the oil is heated by six 2.0 kW, 208 VAC electric heaters to provide thermal energy to warm up the A/F mixture prior to the intake. Once the engine starts, the hot exhaust is used in the ATA heat exchanger to provide the required thermal energy. This transition takes place gradually, as the engine warms up, and at steady state, the heaters are no longer utilized. The required intake thermal energy comes from the waste heat generated by the engine. Figure 2 shows the overall thermal conditioning system including both the LTA and ATA heat exchangers, as installed in the HCCI system.

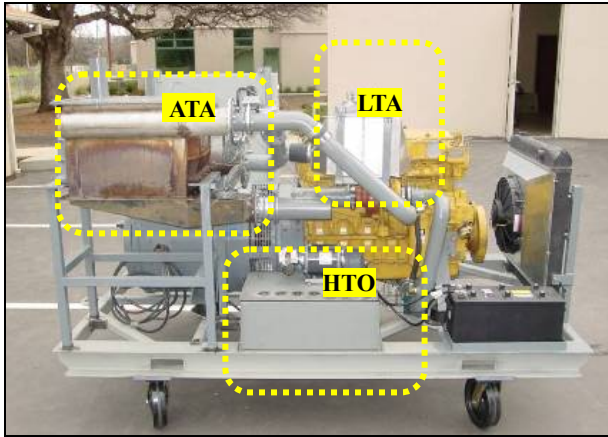


Figure 2 - Thermal Conditioning System Components- ATA Heater Exchanger, LTA Heat Exchanger and HTO Reservoir

Re-configuration of the intake ducting allowed for the use of butterfly valves to control inlet temperature rather than HTO temperature. In future evolutions of this genset, the engine may be started as a spark ignited engine and transitioned to HCCI mode eliminating need for LTA during startup [7,8]. Other starting methods include: starting a diesel engine, on diesel fuel, and then transitioning to carbureted LFG in HCCI mode after about 5 minutes of Diesel mode, ATA heat exchanger reaches operating temperature [7,8].

For optimization of power output and system efficiency, a means to adjust the inlet temperature to each cylinder is required [9]. To supply each cylinder with a slightly elevated or decreased inlet temperature, the ICTC manifold was developed. Figure 3 shows the internal heating mechanism of an individual runner of the ICTC manifold. The main components of the ICTC include: 200 Watt heaters and thermocouple probes. Figure 4 shows the ICTC about to be installed.



Figure 3 - Installed Thermocouple Probe and Electrical Heater Block 2.0 in wide by 6.0 in long



Figure 4 - ICTC Manifold Prior to Installation Showing All Six Port Heaters

The ICTC manifold was modeled after technology pioneered at The University of California at Berkeley as described in appendix A [10]. Further development of the ICTC manifold will incorporate the Fast Thermal Management technologies developed by Ford and by the Lund Institute of Technology [11-13].

INSTRUMENTATION AND CONTROL

Makel Engineering has developed a customized control system to monitor and control engine operation. A host PC/laptop provides a platform for the feedback control system and processes the auxiliary measurements for diagnostics during system testing. Components for control and measurement include thermocouples, mass flow meters, a manifold absolute pressure (MAP) sensor, watt transducer, actuated valves, and data acquisition modules. Other components include soft start and heating elements.

The control system can be broken down into the thermal control system, the fuel control system and the data acquisition system. The main components of the thermal control system are the thermocouple inputs, the relays and an actuated butterfly valve. The main components included in the fuel control system are the air mass flows meter, the fuel mass flow meter, and an actuated control valve. The data acquisition system includes thermocouples, mass flow meters, MAP sensor, tachometer and watt transducer.

To sustain optimal firing conditions, a synchronization of the fuel control system and the thermal control system is executed. When running in HCCI mode, the host PC/laptop performs temperature and fuel flow measurements and responds accordingly. A safety shut down sequence is executed when the conditions are such that the engine may be potentially damaged.

Soft Start A Magnetek soft start (part number RVS-DN) is designed for use with standard three-phase, three-wire, squirrel cage induction motors. It provides a reliable method of reducing the “in rush current” (which can be 9 times the steady state full power current rating of the motor.) and torque during motor start up. The RVS-DN starts the electric motor/generator by supplying a slowly increasing voltage, providing a “soft start” up and smooth electrical acceleration, while drawing the minimum current necessary to ramp up the electric motor/generator the synchronous speed of 1800 RPM.

Safety System The safety system is intended to prevent damage to the engine or hazardous operation of the system, both when supervised by an operator and when running unattended. Events that would trigger a shutdown include: manual emergency stop (E-stop) engaged, host PC crash, overheating, loss of oil pressure, and RPM runaway.

Equivalence Ratio Control The equivalence ratio (ϕ) is defined by Equation 1 [14]:

$$\phi = \frac{(A/F)_s}{(A/F)} \quad \text{Equation 1}$$

Where $(A/F)_s$ is defined as the ratio between Air to Fuel ratio at stoichiometric combustion and (A/F) is the actual Air to Fuel ratio of the engine.

During operation, ϕ is determined by the mass flow of both fuel and air, being computed, logged and displayed real-time by the control system. The fuel control system allows for automatic adjustment of the flow rates. The energy content in the LFG mixture is determined primarily by the methane content, which in turn determines the magnitude of the fuel rate adjustment.

During NG bench testing, the equivalence ratio was set manually with a ball valve. For field testing, a proportional control valve will be utilized to control the equivalence ratio. If ϕ is within the acceptable range, no action is taken. If ϕ is too low, the fuel flow rate is increased, if ϕ is too high, the fuel flow rate is decreased. Utilizing the signal from a methane sensor and control techniques, a fine control will be implemented by actuating the valve that controls the fuel flow.

Thermal Control The control system utilizes a control algorithm to adjust the bulk inlet temperature to the ICTC manifold. The user inputs the desired bulk manifold set temperature, then control system actuates the butterfly valve in the intake line to limit the amount of air fuel charge that passes through the ATA heat exchanger. In conjunction with the bulk heating/cooling, the ICTC manifold has the capability of controlling the inlet temperature to each individual cylinder. The control algorithm for the ICTC is under ongoing development.

HCCI TESTING RESULTS

Testing has consisted of verification of the control electronics and operation of the genset in HCCI mode. After confirming that the system was safe to operate, running the genset in HCCI mode commenced using propane as fuel. Propane as a fuel source led to an understanding of how the genset responded thermally. NG was then utilized as fuel for optimization of the engine output. The project objectives were used as a target for engine output optimization with NG then SLFG as a fuel source.

START UP RESULTS

The engine is capable of making the LTA to ATA heat exchanger transition as well as the propane to NG transition. Figure 5 depicts the typical bulk inlet manifold temperature during the startup process. During startup, the engine spins electrically powered by the induction generator acting as a motor. Once the desired intake temperature is reached, the engine operates on propane fuel for approximately 15 minutes. The LTA heat exchanger provides a bulk manifold set temperature of about 130 Celsius (location "1" on plot). During this time, the ATA heat exchanger is being heated from the hot exhaust gasses. As the LTA to ATA heat exchanger transition takes place, a perturbation in inlet temperature is observed (location "2" on plot). This is due to the positioning of butterfly valves which allow the intake charge to bypass the LTA heat exchanger. The change in bulk manifold temperature does not cause the engine to misfire.

After making the ATA to LTA transition, the bulk manifold temperature is held at approximately 110 Celsius for about 10 minutes while the engine operates steadily on propane as fuel (location "3" on plot). Next, NG is introduced as fuel while the propane fuel is shut off. During the propane to NG transition, the bulk manifold temperature set temperature is changed to 195 Celsius. NG is slowly added to the intake charge and propane flow is slowly decreased until no propane is flowing (location "4" on plot). Finally the engine is operating on NG (location "5" on plot).

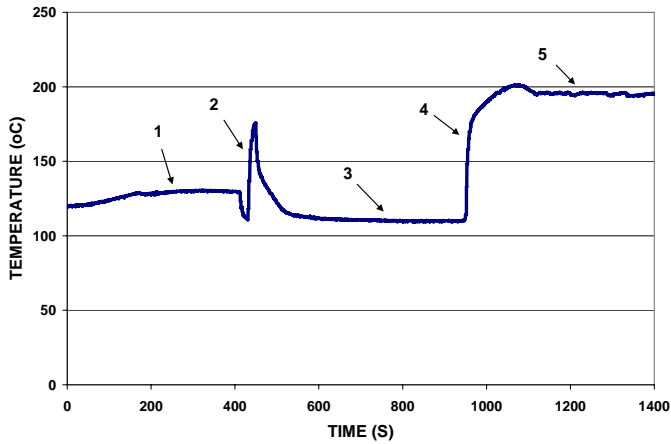


Figure 5 - Bulk Inlet Manifold Temperature During Startup

GENSET ENERGY BALANCE

The main components of the HCCI genset system include: engine, radiator and generator. The components of the subsystem include: HTO oil reservoir, LTA heat exchanger, ATA heat exchanger and turbocharger. A simplified schematic of the HCCI genset is shown in Figure 6 illustrating the power distribution points of the system [15].

The HCCI intake charge requires about 10.0 kW of heating achieve to an ideal intake temperature for combustion to occur. The modified intake supplies the required heat to achieve inlet temperature. This heating is supplied by electrical power during startup and recuperated exhaust heat during steady state operation.

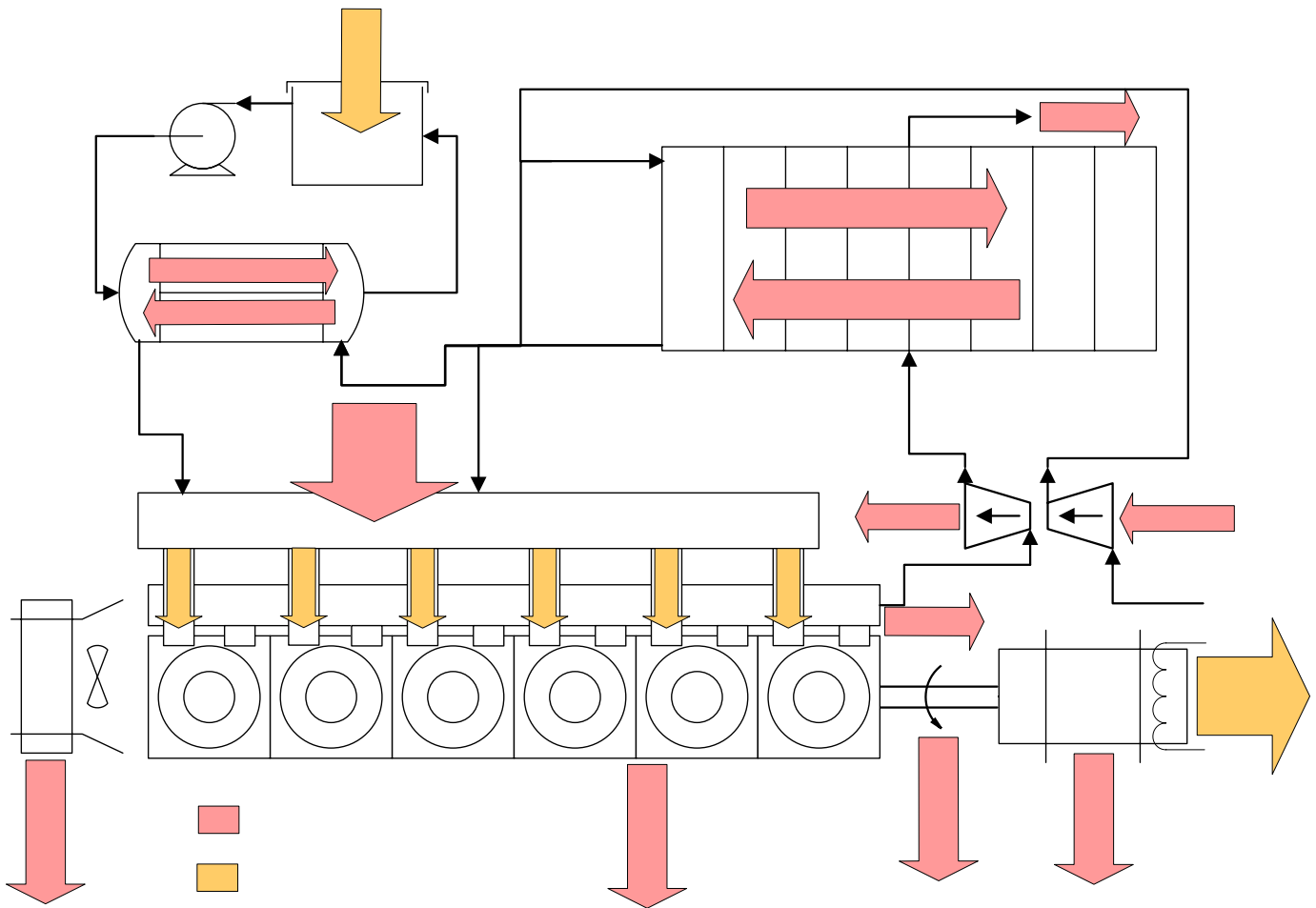


Figure 6 - HCCI Genset Power Distribution Points- Notice the by-pass with control valve of the ATA

Table 3 - Definitions and Typical Values for Power Distribution Points

Sym.	Definition	Value (kW)
P_{HTO} :	Electrical power input to HTO during startup	12.0
$P_{HTO-LTA}$:	Power input from HTO during startup	11.5
$P_{int-LTA}$:	Power added to intake stream during startup	10.0
$P_{T1 \text{ to } T6}$:	Electrical power input to trim heaters	0.0 to 0.4
P_{fuel} :	Power from combustion of fuel	85.0
P_{e-exh} :	Power loss from evacuated exhaust gases pre-turbo and ATA	30.0
P_{e-loss} :	Engine power losses	5.0
P_{cool} :	Power rejected by engine coolant	25.0 to 28.0
$P_{exh-ATA}$:	Power recovered from exhaust stream	17.0
$P_{int-ATA}$:	Power added to intake stream during steady state operation	10.0
P_{exh} :	Power loss from escaping exhaust gases	6.5
P_{turb} :	Power recovered from the turbine side of the turbocharger	6.5
P_{comp} :	Power added to intake stream from turbocharger compressor	6.0
P_{brake} :	Brake power at the engine's crankshaft	27.0 to 30.0
P_{g-loss} :	Power losses associated with the generator	2.0
P_{gen} :	Electrical power output	25.0 to 27.0

The LTA sub-system is comprised of the HTO reservoir, oil pump and LTA heat exchanger. The HTO requires 12.0 kW (six 2.0 kW, 208 VAC electric heaters) of electrical energy (P_{HTO}) for a duration of 1 hour to warm the sub-system. The HTO is pumped through the LTA heat exchanger warming ($P_{HTO-LTA}$) the heat exchanger on the liquid or oil side. The incoming air on the air side of the heat exchanger is then warmed ($P_{int-LTA}$) by the heat exchanger. Testing has determined that the LTA sub-system is approximately 65% effective. About 650 Watts of power heats the intake charge per 1.0 kW of electrical heating at a mass flow rate of about 280 kgph. The electrical trim heaters in the ICTC manifold provide up to 400 W ($P_{T1 \text{ to } T6}$) of additional heating per cylinder.

The BTU value of the NG delivered to MEI's testing facility changes daily. Figure 7 depicts a plot of the daily BTU value for the recent HCCI genset optimization. For engineering computations, the daily BTU value was converted to a lower heating value of in kilojoules per kilogram. The average lower heating value has been 47,200 kJ/kg. Operating at an equivalence ratio of 0.33 and an inlet pressure of 1.5 atm, the mass flow of NG is about 6.5 kgph. The combustion of NG

at this flow rate releases approximately 85.0 kW of power (P_{fuel}).

Not all of this power is converted directly into electrical power. About 30.0 kW of this energy (P_{e-exh}) is evacuated as hot exhaust gases. Other engine power losses account for about 5.0% or 5.0 kW of the power from the fuel. These losses (P_{e-loss}) include: radiation, lubrication system and other small losses.

A large part of this heat is lost to the piston chamber walls. To prevent the piston walls from becoming too hot, the cooling system removes heat through the circulation of engine coolant. The cooling system is capable of removing from 25.0 to 28.0 kW (P_{cool}) depending on fan speed.

At a mass flow rate of about 320 kgph, about 17.0 kW of power ($P_{exh-ATA}$) is recovered from the exhaust stream providing the required 10.0 kW of power ($P_{int-ATA}$) to the intake stream. About 6.5 kW is released to the atmosphere (P_{exh}) in the exhaust gases leaving the ATA. At steady state the ATA is approximately 65% effective.

The turbocharger also recovers some of the power loss from the evacuated exhaust gases. The turbine side of the turbocharger converts about 6.5 kW exhaust heat into mechanical energy to drive the compressor side of the turbocharger. The compressor side of the turbocharger adds about 6.0 kW of heat to the intake charge (P_{comp}). See steady state operation results for turbocharger optimization.

About 27.0 to 30.0 kW of the power available from the fuel remains at the engine crankshaft defined as engine brake power (P_{brake}). The electric generator is very efficient. The nameplate efficiency rating on the Century 150kW motor is 93%. Power loss thru the generator (P_{g-loss}) is assumed to be about 7% or 2.0 kW of the brake power at the engine crankshaft. Finally, the genset outputs from 24.0 to 27.0 kW of electrical power (P_{gen}).

During steady operation, the ATA heat exchanger recuperates more than the required 10.0 kW of heating. To maintain a desired intake temperature, a portion of the intake charge bypasses the ATA. A motorized butterfly valve in the intake system prior to the ATA is "dithered" to control bulk manifold inlet temperature. A control algorithm with programmable dead band and response time has allowed for a bulk inlet temperature to be controlled to within 1.0 degree Celsius.

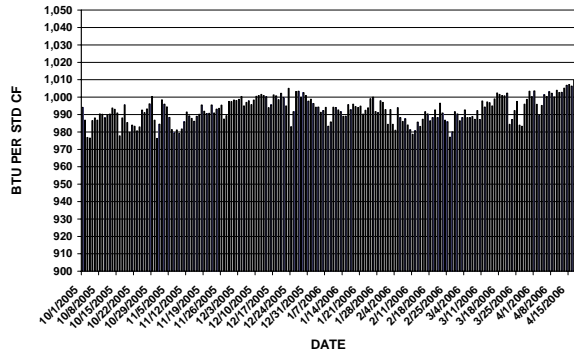


Figure 7 - Daily BTU Value Natural Gas Delivered to MEI for the 14 months of Natural gas testing

LANDFILL GAS COMPOSITION

Tapping into the existing flaring station at the NRL, a delivery manifold to port the landfill gas over to the HCCI genset was installed. The methane, nitrogen and carbon dioxide concentrations of the LFG from NRL have been monitored weekly for the past several months. The flare flow rate has varied from about 675 CFM to 1000 CFM. The methane concentration has ranged from 35% to 60%. The carbon dioxide concentration has varied from 25% to 30%. Figure 8 shows the methane, carbon dioxide and nitrogen concentrations for LFG sampling. The gas sampling method used is not capable distinguishing nitrogen from air. For sampling, the balance gas was assumed to be nitrogen. The most recent data has indicated about 40% methane, 30% nitrogen and 30% carbon dioxide. The recorded landfill gas compositions listed in Table 4 indicate that the ratio of methane to carbon dioxide varies from 1.3:1 to 2.4:1 and the ratio of methane to nitrogen varies from 1.1:1 to 4:1.

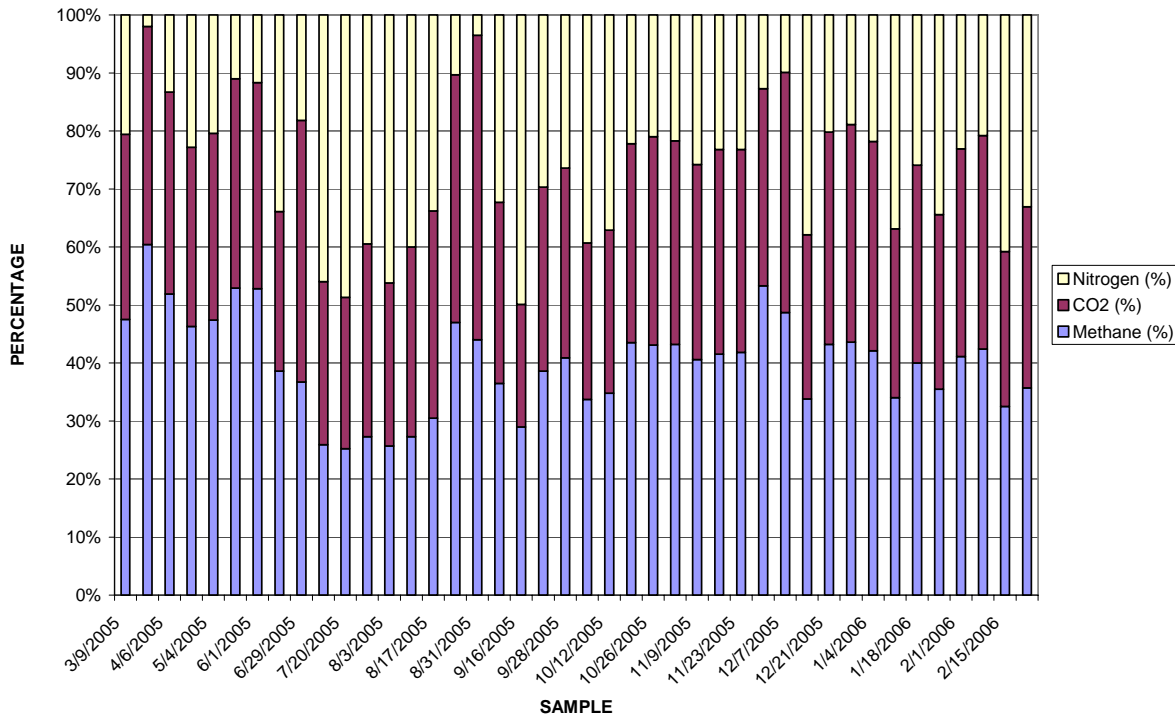


Figure 8 - Respective Methane, Carbon Dioxide and Nitrogen concentrations found in the LFG Samples Pulled from Delivery Manifold at NRL

Table 4 - Measured Landfill Gas Compositions

FUEL	CH ₄	CO ₂	N ₂	(CH ₄ : CO ₂)	(CH ₄ : N ₂)
Most Methane	60	25	15	2.4:1	4:1
Typical	40	30	30	1.3:1	1.3:1
Least Methane	35	25	30	1.4:1	1.1:1

For SLFG testing, MEI used a worse case of scenario for high carbon dioxide concentration and also for high nitrogen

concentration in the LFG. Figure 9. depicts an example of how the SLFG fuel mixture was delivered to the engine for SLFG performance testing.

Diluent gas ratios for CH₄: CO₂ and CH₄: N₂ of 1.2:1, 1.5:1 and 1.9:1 were tested. The remaining diluting gas was assumed to be air in both cases. While the engine was operated with all of these concentrations, additional optimization testing was performed with the ratios of 1.5:1 methane balance carbon dioxide to meet the project goals for NO_x emissions.

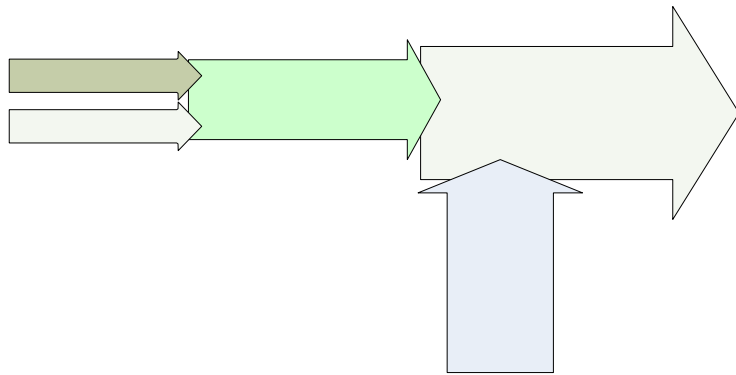


Figure 9 - Simulated Landfill Gas Intake Diagram

STEADY STATE OPERATION RESULTS

After validating the system start-up procedure, optimization of the system outputs continued working towards the program goals. Optimization steps included:

- Establishing a baseline system efficiency
- Increasing power output through the development the turbocharger

- Optimizing the intake system
- Determining the inlet conditions and equivalence ratio that optimized NO_x emissions in relationship to efficiency

System efficiency is defined as the fuel to electricity power ratio for the system. It is computed using Equation 2 [14]:

$$\eta = \frac{(P_{gen})(3600)}{(m_{fuel})(LHV_{fuel})} \quad \text{Equation 2}$$

Where (P_{gen}) is the electrical power output in kW, (m_{fuel}) is the mass flow of the fuel in kilograms per hour and (LHV_{fuel}) is the lower heating value of the fuel in kilojoules per kilogram.

Brake power output is defined as the output available at the output of the engine crankshaft. Brake thermal efficiency (BTE) is defined in Equation 3 [14]:

$$\eta = \frac{(P_{brake})(3600)}{(m_{fuel})(LHV_{fuel})} \quad \text{Equation 3}$$

Where (P_{brake}) is the available power output in kW at the crankshaft, the mass flow of the fuel (m_{fuel}) is in kilograms per hour and (LHV_{fuel}) is the lower heating value of the fuel in kilojoules per kilogram.

Once steady conditions are reached, the system meets the stability goals of less than 10% variation in system stability. To verify stability, efficiency was plotted over a one hour period, see Figure 10. Notice less than 3% variation.

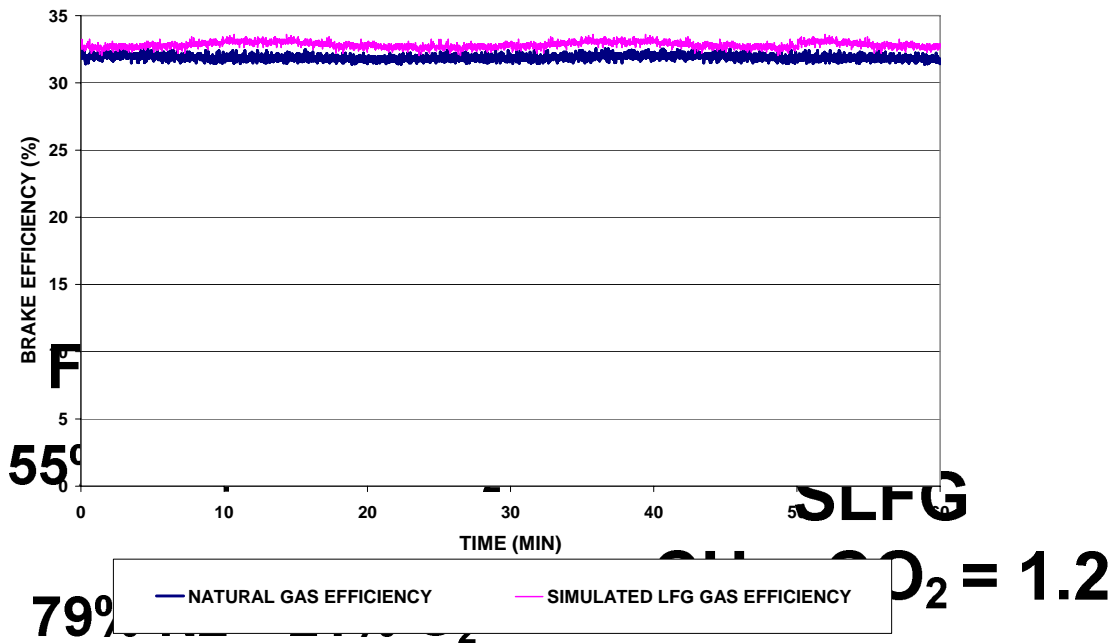


Figure 10 - System Stability is Good

ADDITIONAL DILUTION

Efficiency and Power Output After about 80 hours of testing, MEI successfully achieved steady operation in HCCI mode while operating on NG. It requires about 60 minutes to achieve these conditions. Efficiency and power data obtained during this time was used to improve the system. Modifications to the system allowed for improved outputs; working towards the project goals. Modifications to the HCCI genset were developed around the intake system and engine block/pistons. The HCCI genset underwent five major modifications. These five engine configurations with their corresponding maximum efficiencies and power outputs are summarized in Table 5. The original engine configuration (configuration “A”) was important stepping stone to the current design. It validated that the system was capable of operating in HCCI mode with NG as a fuel source. It also served as a test platform for the electronics and instrumentation. The best efficiency was found to be 18.0% while producing about 15 kW of electrical power.

Potential sources for the lower than expected efficiency were identified as the following: non-optimal ignition timing of all six cylinders, lower than expected compression due to leakage around piston rings and higher than expected friction in the engine. Additions included the ICTC manifold as well as replacing the engine block with a new short block (configuration “E”) consisting of new pistons, rings, and crank shaft. Re-building the HCCI genset ensured that potentially incorrect conclusions based unique problems with the original engine block. After this final modification to the genset, the efficiency numbers were 5% to 10% improved. The engine currently is capable of achieving 35.0% BTE and producing about 27.0 kW utilizing NG as fuel.

Table 5 - Engine/Genset Configuration and Output Summary

Config.	Description	BTE (%)	Power (kW)
A	Original configuration	19.3	15.3
B	Original engine with modified intake simple	20.6	18.2
C	Original engine with ICTC intake	24.8	21.5
D	Original engine with modified inlet to ICTC	26.0	22.2
E	Re-built engine with ICTC intake (Current)	35.0	26.9

After optimizing the engine for operation on NG, the most favorable inlet conditions for running on SLFG were developed. Efficiency and power data obtained during this time was used to improve the system. Table 6 summarizes the peak efficiency and power output for the optimized carbon dioxide and nitrogen concentrations used to simulate LFG. The engine currently is capable of achieving about 34.0% BTE (about 31.5% system efficiency) and producing about 29.0 kW while operating on SLFG.

Table 6 - Engine/Genset Peak Output Summary

FUEL	BTE(%)	Power (kW)
Natural Gas	35.0	26.9
SLFG 1.5:1 (CH ₄ : CO ₂)	33.9	28.9
SLFG 1.5:1 (CH ₄ : N ₂)	33.2	29.1

Turbocharger Optimization Improvement of power output and system efficiency was achieved through the development and implementation of an appropriate turbocharger. As shown in Figure 11 and Figure 12, a turbocharger has the following components: compressor housing, compressor impeller, bearing housing, turbine shaft and turbine housing.

Figure 13 indicates pressures P_1 , P_2 , P_3 and P_4 flowing into and out of a turbocharger. The pressure of the intake charge coming from the carburetor and entering the compressor side of the turbocharger is defined as P_1 . The pressure of the intake charge leaving the compressor side of the turbocharger heading toward the engine intake is defined as P_2 . The pressure of the exhaust gases prior to entering the turbine side of the turbocharger is defined as P_3 . The pressure of the exhaust gases prior to entering the turbine side of the turbocharger is defined as P_4 . The MAP is recorded in the engine intake. These pressures were measured and used to compute the performance parameters of the turbocharger.



Figure 11 - Compressor Housing and Turbine-Housing



Figure 12 - Compressor Impeller, Bearing Housing and Turbine Shaft

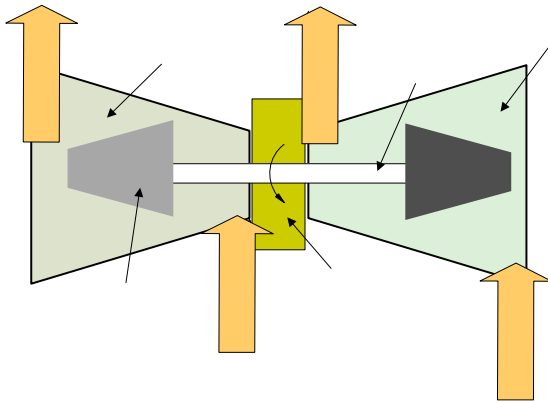


Figure 13 - Turbocharger Diagram

Each turbocharger investigated was characterized by the following performance parameters: air flow, pressure ratio, boost and back pressure. Air flow, measured in kilograms per hour, quantifies the amount of air turbocharger pulls through the intake. Boost is the amount of pressure increase as measured by the manifold absolute pressure sensor in the engine intake. Pressure ratio is the pressure increase across the compressor side of the turbocharger. Back pressure is the amount of pressure the turbine side of the turbocharger exerts on the engine exhaust manifold. Pressure ratio (P_r) and back pressure (P_b) are computed in Equation 4 and Equation 5 [14]:

$$P_r = \frac{P_2}{P_1} \quad \text{Equation 4}$$

$$P_b = \frac{P_3}{P_4} \quad \text{Equation 5}$$

There are thousands of different turbine, compressor, and compressor impeller combinations. Testing started with the stock CATERPILLAR turbocharger (iteration #1) designed for

use when operating on diesel fuel. After poor results from this turbocharger, it was decided to work with a turbocharger manufacturer to develop a suitable turbocharger combination for running in HCCI mode. Working as a development project, a customized turbocharger manufacturing company agreed to help with the development of a turbocharger for optimal use in HCCI mode of operation.

The first turbocharger iteration was sized for a diesel engine with about half the displacement or 3.0 L of the CAT 3116 engine. Determining the optimal turbine housing and compressor housing with compressor impeller and turbine shaft required another six configurations. Table 7 summarizes the results for each of the studied turbocharger arrangements.

Increased boost pressure allows more fuel to be present per combustion stroke due to an increase in the density of the intake charge. Increased air flow is a direct effect of having a higher boost pressure. Increasing these parameters leads to higher power output. It was determined that for optimal power output, the engine would need to be operating with a boost of 200 kPa passing about 450 kilograms per hour of air. Working towards this goal, a boost pressure of about 150 kPa moving about 335 kilograms per hour of air has been achieved.

Table 7 - Turbocharger Iteration Summary

Turbo Iter.	Air Flow (kg/hr)	Boost (kPa)*	Press Rat. (P_r)**	Back Press. (P_b)
1	227.8	110	1.12	1.43
2	253.6	106	1.15	1.29
3	245.2	129	1.31	1.44
4	269.2	143	1.44	1.70
5	276.5	151	1.53	1.84
6	302.1	142	1.49	1.85
7	286.0	131	1.44	1.68
8	335.9	148	1.61	1.82

* Based on MAP

**Based across turbo

Intake Temperature Optimization The intake system was modified to improve engine performance. The most significant modification was the development of the ICTC manifold. Further improvements included the re-routing of the intake charge into the ICTC manifold from the top rather than from the end.

The ICTC manifold was designed for a 15-20 degrees Celsius temperature increase from cylinder to cylinder. Figure 14 shows a typical temperature response for the incoming intake charge when the rheostat was turned from 50% to 100% power on Cylinder #1, while keeping the cylinders #2 through #6 at 50%. A 50% increase in power lead to about a 10 degree Celsius increase in inlet temperature for Cylinder #1. The intake to cylinder #2 receives some of the beneficial heating when cylinder #1 is heated.

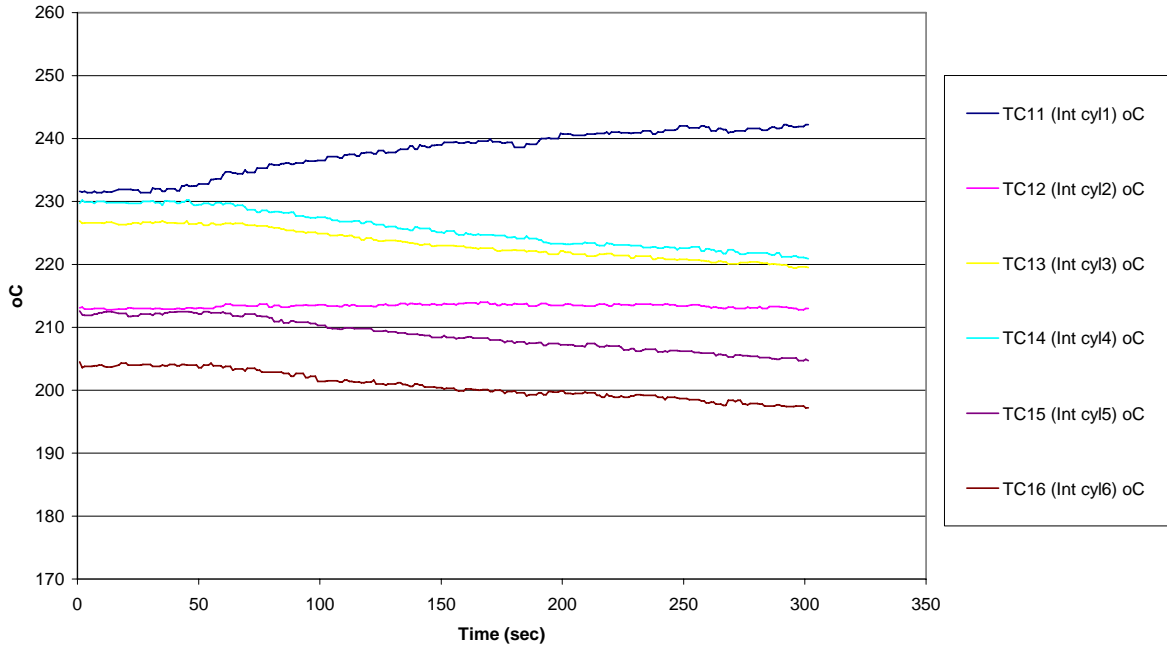


Figure 14 - ICTC Temperature versus Time Response -- 50% Increase for Cylinder #1

Figure 15 shows the individual cylinder temperature response when the rheostat was turned from 100% to off for Cylinder #1 while the other cylinders were kept at 50%. As indicated in the plot, a transition from full power to off, led to about 25 degree Celsius decrease in inlet temperature for cylinder #1. While optimizing the running conditions, the header bulk inlet temperature was set slightly higher than

optimal inlet temperature to allow for minimal heat addition to the individual cylinders. For example, cylinders 1-3 may need 50% power while cylinders 4-6 may need 20% and cylinder #6 none, when the bulk inlet temperature was set to the optimal firing temperature for cylinder #6.

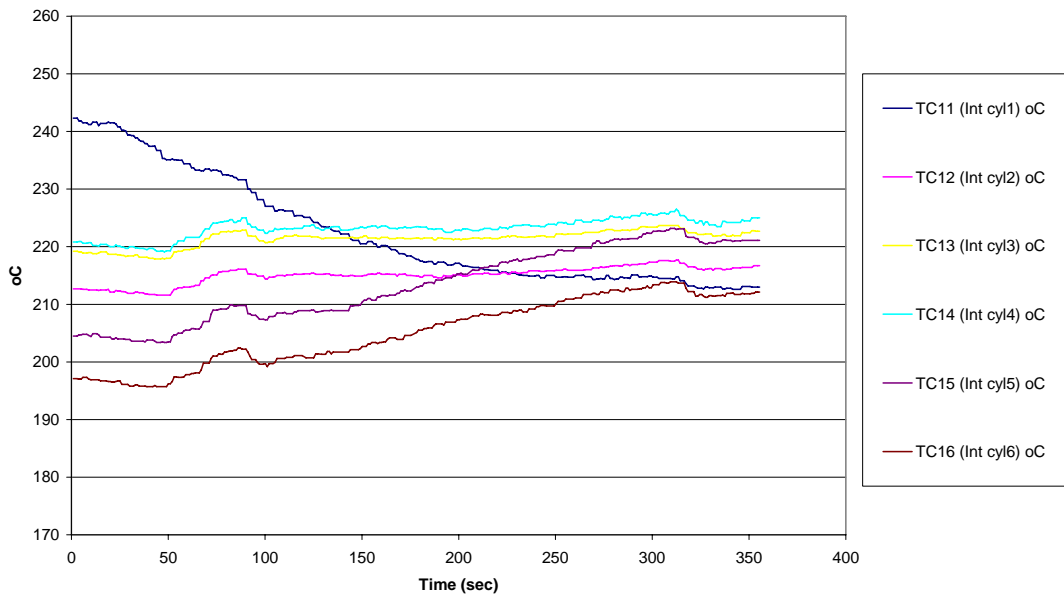


Figure 15 - ICTC Temperature Versus Time Response -100% Decrease for Cylinder #1

System Optimization and Emissions Output

Without the utilization of a turbocharger, the HCCI genset was unable to sustain steady operation. Working through several turbocharger iterations has afforded the optimization the power and efficiency output while mapping the emissions output of the HCCI genset. The effect of an optimized turbocharger has

been higher boost pressure at the engine intake manifold. When turbocharger iteration #8 was operated at about 140 kPa, a BTE of about 31.0% was recorded. When the same turbocharger was operated at about 150 kPa, the BTE was 35.0%. Figure 16 shows the effect of boost pressure on system efficiency for turbocharger iteration #8.

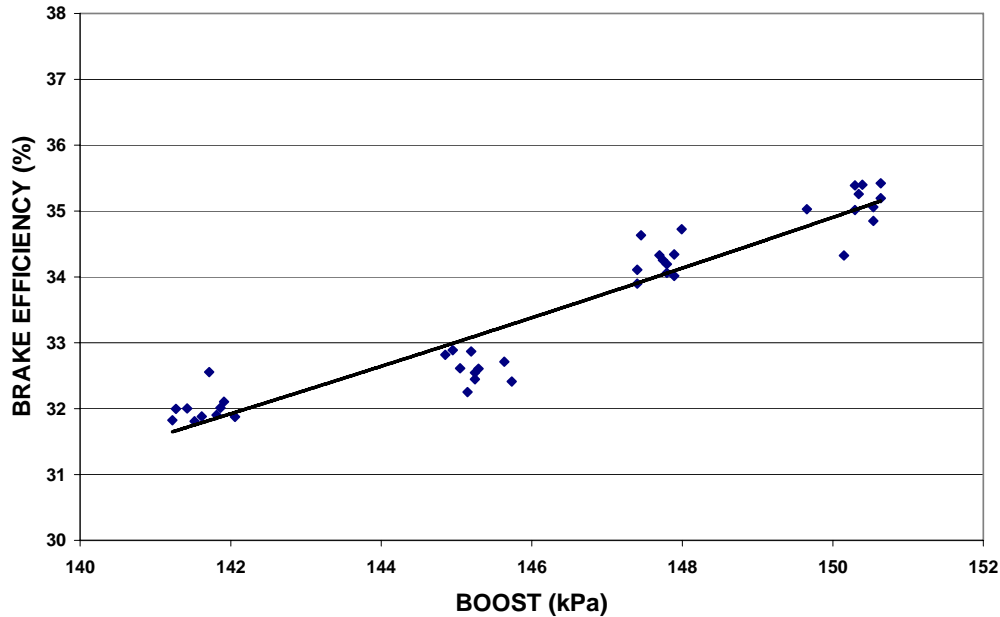


Figure 16 - HCCI Performance – Turbocharger Boost versus Brake Efficiency

All optimization testing was done while the engine was under a 70 kW load being fed by both the grid and the HCCI genset. Using NG, the BTE is about 33.0% while producing about 27.0 kW of power; however under these operating conditions the NO_x emissions did not meet program goals. By lowering the equivalence ratio and increasing the inlet temperature MEI was able to achieve a BTE of about 33.0% while producing 24.0 kW of power and generating less than 4.0 ppm NO_x emissions. Table 8 summarizes the operating conditions which produced these results.

Table 8 - HCCI Performance –Operating Conditions for Peak Efficiency and Emission Levels for Natural Gas

INLET CONDITION			OUTPUT		
PHI	INTAKE MAN. TEMP(oC)	MAP (kPa)	POWER OUTPUT (kW)	BTE (%)	NO _x LEVEL (ppm)*
0.36	160	145	26.9	35.0%	9.2
0.33	165	146	23.9	33.0%	3.6

*All reported NO_x are corrected for 15.0% Oxygen

Using SLFG, the peak BTE was about 34.5% while producing about 27.0 kW of power; similarly to NG operation,

the NO_x emissions did not meet program goals. Using the engine tuning knowledge gained by operating on NG, a peak BTE of about 33% was achieved while producing about 26.0 kW of power, generating about 5.0 ppm NO_x emissions. Table 9 summarizes the operating conditions which produced low NO_x emissions while operating on SLFG.

Table 9 - HCCI Performance –Operating Conditions with Low Emission Levels for Simulated Landfill Gas

FUEL	INLET CONDITION			OUTPUT		
	PHI	INTAKE TEMP (oC)	MAP (kPa)	POWER OUTPUT (kW)	BTE (%)	NO _x LEVEL (ppm)
1.2:1 (CH ₄ : CO ₂)	0.35	185	146	25.9	32.5%	5.4
1.5:1 (CH ₄ : CO ₂)	0.35	185	142	25.5	30.8%	4.7
1.9:1 (CH ₄ : CO ₂)	0.38	175	143	27.6	32.9%	5.2
1.2:1 (CH ₄ : N ₂)	0.36	170	137	24.4	31.2%	5.7

1.5:1 (CH ₄ : N ₂)	0.36	170	135	23.2	30.8%	4.7
1.9:1 (CH ₄ : N ₂)	0.38	160	140	26.2	31.7%	5.4

Figure 17 shows the NO_x emissions as a function of equivalence ratio for HCCI operation on NG. As anticipated, the NO_x emission levels decrease at lower equivalence ratios. Figure 18 shows the NO_x emissions as a function of equivalence ratio for NG and for methane-carbon dioxide simulated landfill gas. Figure 19 shows the NO_x emissions as a function of equivalence ratio for NG and for the methane-nitrogen simulated landfill gas. The NO_x emission levels for simulated landfill gas were similar to that of NG.

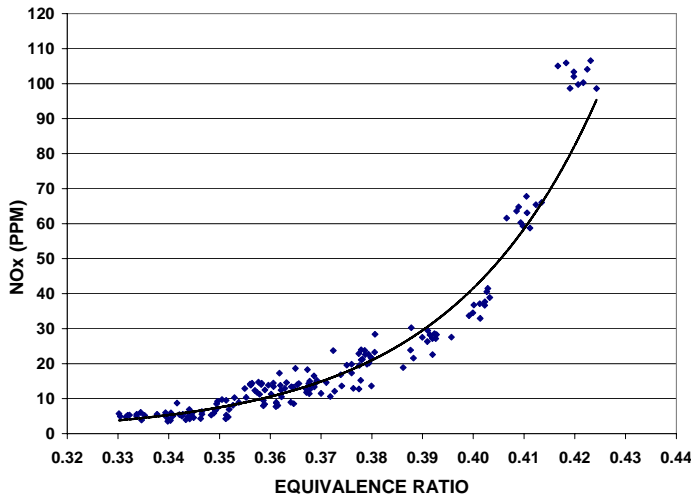


Figure 17 - HCCI Performance on NG –Remarkably Low NO_x Emission Levels versus Equivalence Ratio

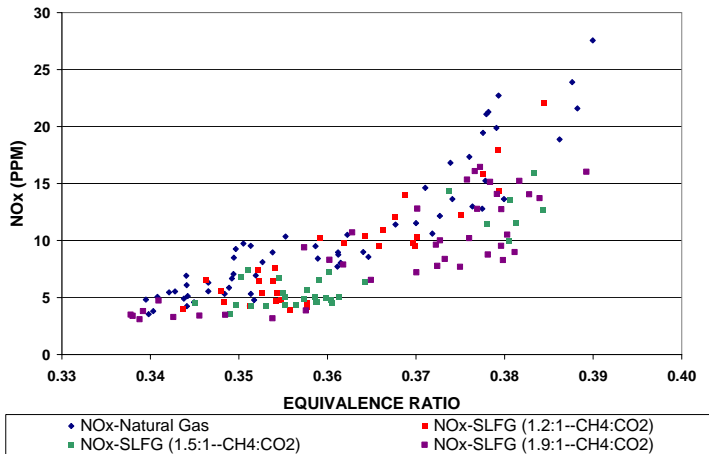


Figure 18 - HCCI Performance on SLFG – Carbon Dioxide Diluent, NO_x Emission Levels Versus Equivalence Ratio

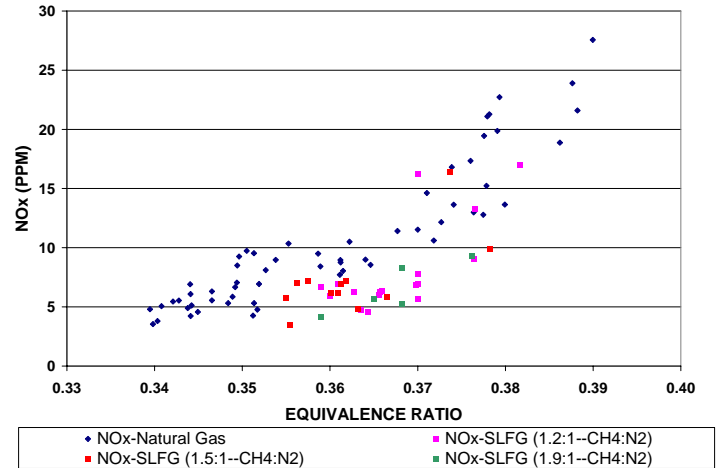


Figure 19 - HCCI Performance on SLFG – Nitrogen Diluent, NO_x Emission Levels and Equivalence Ratio

Other exhaust gas species were measured. These gases include Carbon Dioxide (CO₂), Oxygen (O₂), Carbon Monoxide (CO), and Unburned Hydrocarbons (UHC). These exhaust constituents were measured with and without a 3-way catalytic converter in the exhaust stream. Table 10 lists the levels of other exhaust gas constituents which were recorded while operation in HCCI mode under nominal operating conditions without the utilization of a catalytic converter. NG and then SLFG with a CO₂:CH₄ ratio of 1.9:1 was utilized as fuel for this testing.

Table 10 - HCCI Performance –Other Exhaust Gas Species-- Without Catalytic Converter

FUEL	ENGINE OUTPUT		EXHAUST GAS				
	POW. (kW)	BTE (%)	O ₂ (%)	CO ₂ (%)	CO (ppm)	UHC (ppm)	NO _x (ppm)
NG	23.9	33.0%	~16.0	~7.5	<90.0	<150	~3.6
SLFG	25.9	33.0%	~16.0	~12.0	<90.0	<150	~4.3

Further testing with a catalytic converter installed in the exhaust stream was performed to evaluate the reduction in CO and UHC. No reduction in NO_x was measured with the catalytic converter installed; however, a significant reduction in CO and UHC was recorded. No measurable reduction in engine performance was noted. Table 11 summarizes the levels of other exhaust gas constituents recorded while utilizing NG and SLFG as a fuel source.

Other engine performance parameters were computed. These include: brake power, torque, BTE, specific power and output per displacement. Table 12 summarizes these parameters while using NG and SLFG as fuel.

Table 11 - HCCI Performance –Other Exhaust Gas Species—With- Catalytic Converter

INLET COND.		ENGINE OUTPUT		EXHAUST GAS				
EQUIV. RATIO	INTAKE TEMP(oC)	POWER (kW)	BTE (%)	O ₂ (%)	CO ₂ (%)	CO (ppm)	UHC (ppm)	NO _x (ppm)
NG								
0.34	165	26.8	33.1	15.4	~7.5	<5.0	5.9	3.8
0.36	165	26.9	33.4	15.4	~7.5	<5.0	6.3	6.6
0.38	165	27.2	32.2	15.4	~7.5	<5.0	8.3	9.4
SLFG								
0.35	175	25.6	28.3	15.3	~11.0	<5.0	7.8	4.4
0.38	175	26.5	29.5	15.4	~11.5	<5.0	9.7	5.2
0.41	175	28.3	31.7	15.3	~11.0	<5.0	9.9	7.6

Table 12 - Other Engine Performance Parameters for NG and SLFG

FUEL	INLET CONDITION			OUTPUT						
	PHI	INTAKE TEMP (oC)	MAP (kPa)	POWER OUTPUT (kW)	BRAKE POWER (kW)	TORQUE -[N-M]	BTE (%)	NO _x LEVEL (ppm)	SP (KW/M ²)	OPD (KW/L)
NG	0.36	160	1.45	26.9	28.9	153.3	35.0%	9.2	556.2	4.4
NG	0.33	165	1.46	23.9	25.7	184.5	32.9%	3.6	493.7	3.9
SLFG-1.2:1 (CH ₄ : CO ₂)	0.35	185	146	25.9	27.9	147.9	32.6%	5.4	536.6	4.2
SLFG-1.5:1 (CH ₄ : CO ₂)	0.35	185	142	25.5	27.4	145.6	30.8%	4.7	528.3	4.2
SLFG-1.9:1 (CH ₄ : CO ₂)	0.38	175	143	27.6	29.6	157.2	32.9%	5.2	570.5	4.5
SLFG-1.2:1 (CH ₄ : N ₂)	0.36	170	137	24.4	26.3	139.3	31.1%	5.7	505.4	4.0
SLFG-1.5:1 (CH ₄ : N ₂)	0.36	170	135	23.2	24.9	132.2	30.7%	4.7	479.5	3.8
SLFG-1.9:1 (CH ₄ : N ₂)	0.38	160	140	26.2	28.2	149.3	31.7%	5.4	541.8	4.3

CONCLUSIONS AND RECOMMENDATIONS

Initial testing allowed for optimization of the HCCI engine. By working through the several configurations, the necessary operating conditions to meet the program goals were established. Utilizing NG for this “tuning” of the engine has allowed for testing to continue using simulated landfill gas. Expanding the understanding of HCCI mode of engine operation has allowed for the transition from NG to SLFG and eventually landfill gas as a fuel source.

Operating with NG as fuel, a 35.0% BTE was achieved while producing about 29.0 kW of electrical power. However, at these conditions, the goal of less than 5.0 ppm on NO_x in the exhaust stream was not met. When the HCCI engine was operated with slightly lower equivalence ratio, the emissions goal of less than 5.0 ppm of NO_x was reached. The BTE was about 33.0% while producing about 26.0 kW of electrical power under these conditions. The amount of unburned hydrocarbons and carbon monoxide in the exhaust stream were below 10.0 ppm and 5.0 ppm respectively with a 3-way catalytic converter installed.

Operating with simulated landfill gas as fuel, a 33.0% BTE was achieved while producing about 26.0 kW of electrical power. At these conditions, the emissions goal of less than 5.0 ppm on NO_x in the exhaust stream was met. The genset is capable of achieving 34.0% BTE producing slightly higher NO_x emissions.

While the HCCI genset is on target for meeting project goals while operating on NG and SLFG as fuel, a few design modifications could enhance engine performance. Prospective improvements to the HCCI genset include:

1. More appropriately sized generator (75 or 80 kW rather than 150kW)
 - Less inertia to overcome at startup
2. Larger diameter intake ducting
 - A large diameter on the intake ducting would reduce pressure drop from the landfill to the engine
3. Instrumented engine head
 - The addition of in-cylinder instrumentation (ION SENSING) would allow for a more accurate determination of cylinder firing.
4. Proportional valve on fuel intake line
 - Automated control of the equivalence ratio could be achieved through the implementation of a proportional control valve on the fuel intake line.
5. Larger engine (6.6L currently)
 - Moving to a larger engine would allow for increased power output and likely increased efficiency, greater than 40%

ACKNOWLEDGMENTS

We gratefully acknowledge the support provided by the California Energy Commission specifically Dr. Valentino Tiangco, program manager.

REFERENCES

- [1] Aceves, S. M., Flowers, D., Martinez-Frias, J., J. R. Smith, J.R, Dibble, R. W., Au M., and Girard, J. W., 2001, “HCCI combustion: analysis and experiments” SAE Pare No. 2001-01-2077.
- [2] Aceves, S.M., Smith, J. R., Westbrook, C. K., and Pitz, W. J., 1999, “Compression ratio effect on methane HCCI combustion,” *Journal of Engineering for Gas Turbines and Power*, 121:569-574.
- [3] Fiveland, S. B and Assanis, D. N., 2000, “A four-stroke homogeneous charge compression ignition engine simulation for combustion and performance studies,” SAE Paper No. 2000-01-0332.
- [4] Martinez-Frias, J., Aceves, S. M., Flowers, D. L., Smith, J. R., and Dibble, R. W., 2001, “Equivalence ratio-EGR control of HCCI engine operation and the potential for transition to spark-ignited operation,” SAE Paper No. 2001-01-3613.
- [5] Aceves, S.M., Flowers, D. L., Martinez-Frias, J., Smith, J. R., Westbrook, C. K., Pitz, W. J., Dibble, R. W., Wright, J. F., Akinyemi, W. C., and Hessel, R. P., 2001, “A sequential fluid-mechanic chemical-kinetic model of propane HCCI combustion,” SAE Paper No.2001-01-1027.
- [6] Dec, J. E., 2002, “A computational study of the effects of low fuel loading and egr on heat release rates and combustion limits in HCCI engines,” SAE Paper No. 2002-01-1309.
- [7] Souder, J. S., 2004, “Closed loop control of a multi-cylinder HCCI engine,” PhD Thesis, University of California at Berkeley, Berkeley, CA.
- [8] Flowers, D., Aceves, S. M., Martinez-Frias, J., Smith, J. R., Au, M. Y., Girard, J. W., and Dibble, R. W., 2001, “Operation of a four-cylinder 1.9 l propane-fueled homogeneous charge compression ignition engine: Basic operating characteristics and cylinder-to cylinder effects,” SAE Paper No. 2001-01-1895.
- [9] Martinez-Frias, J., Aceves, S. M., Flowers, D. L., Smith, J. R., and Dibble, R. W., 2000, “HCCI engine control by thermal management,” SAE paper No.2000-01-2869.

- [10] Gans, William L., 2001, "Control of a Multi-cylinder Homogeneous Charge Compression Ignition Engine," Masters Thesis, University of California at Berkeley, Berkeley, CA.
- [11] Yang, J., Culp, T., and Kenney, T., 2002, "Development of a gasoline engine system using HCCI technology the concept and the test results." SAE Paper No. 2002-01-2832.
- [12] Christensen M. and Johansson. B., 1998, "Influence of mixture quality on homogeneous charge compression ignition," SAE Paper No.982454.
- [13] Hiltner, J., Agama, R., Mauss, F., Johansson, B., and Christensen, M., 2000, "HCCI operations with natural gas: Fuel composition implications," In Proc. of the ASME ICE Fall Technical Conference, volume 35, pages 11-19.
- [14] Pulkrabek, W.W., 1997, "Engineering Fundamentals of the Internal Combustion engine," Prentice Hall Upper Saddle River, NJ, Chap. 2,3 and 9.
- [15] Turcotte, D., and Sheriff, F., 2002, "Efficient use of Gensets Through Proper handling of excess Heat," CANMET-Energy Diversification Research laboratory, Varennes QC, Canada.

APPENDIX A

A.1 Introduction

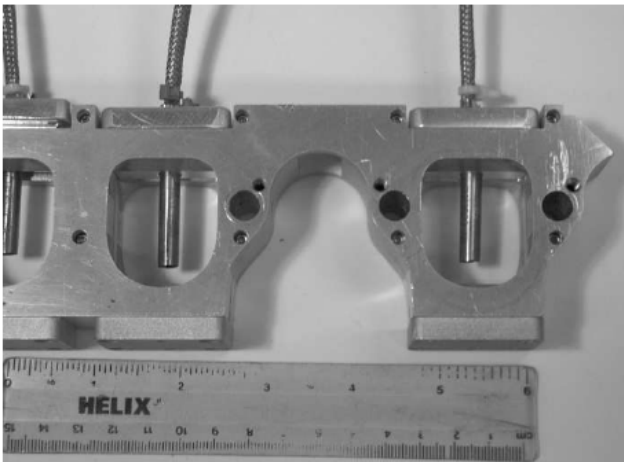
The engine used for the experiments in this investigation was a 1.9L, 4 cylinder Volkswagen TDI. The TDI, Turbocharged Diesel Injected engine, is a diesel engine used in the Passat 1995 model year sedan. In HCCI mode, the engine was run with propane naturally aspirated, without a turbocharger. Propane fuel was steadily flowed 1 meter upstream of the intake manifold to establish homogeneity of the fuel and air. Experiments were conducted at the Combustion Analysis Laboratory at The University of California – Berkeley.

A.2 Intake Apparatus

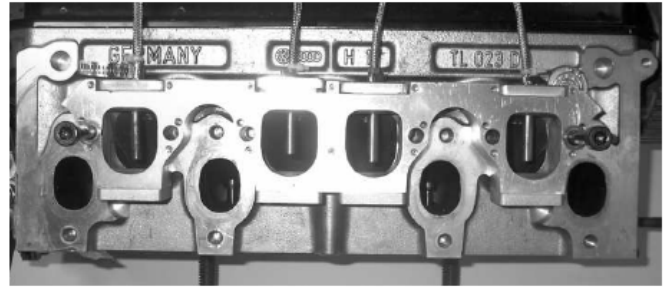
To explore the individual cylinder intake heating as a control technique, intake heaters were mounted at the intake ports of the engine. The intake heaters were made by Fast Heat, and were supplied with a maximum of 100W AC voltage using 4 Variable

AC input devices. The heaters were mounted in a custom intake manifold, pictured below (Figure A1), along with the heaters. OEM Glow plugs were also mounted in the engine.

The glow plugs were used to examine their effect on cylinder heating, and were supplied with 12 Volts from a power supply.



(a) intake heaters



(b) cylinder head with heaters

Figure A1: Intake Heater setup. Figure (a) shows the individual heaters mounted in the intake manifold spacer, and figure (b) shows the intake spacer mounted on the cylinder head with the heaters. Notice the heaters protruding into the intake ports. Heater length is approximately 1.5 inches (38 mm)

A.3 Cylinder Balancing

Ideally, every cylinder within an engine should get the same amount of charge mass (fuel and air) per stroke, have the same compression ratio, and each cylinder should be maintained at identical temperature. Unfortunately, that scenario is not realized in real engines. The failure to align the temperatures, compression ratios, and charge masses of the cylinders results in different pressures and combustion timing (SOC) between the cylinders. This is known as a balancing problem, or an unbalanced engine. Balancing of a multicylinder engine is an important problem. Size and cost constraints dictate many aspects of internal combustion engine design. Involved in the inevitable tradeoffs that take place between ideal engine performance and manufacturing reality are the engine intake and coolant systems. Together, these multi-component systems are responsible for the control of the operating conditions of the engine: the temperature of the cylinder walls and the inlet air distribution. A typical pressure trace for a HCCI engine shows different peak pressures for each cylinder (Figure A2). These pressure differences are the manifestations of an unbalanced engine. Referring to Figure A1, the difference in timing (measured on the horizontal axis in Crank Angle Degrees) and pressure (measured on the vertical axis in bar) between cylinders is obvious.

The engine balancing problem is more than idle perfectionism since the temperatures and pressures inside a Diesel CI engine are much higher than a SI engine. If certain cylinders within an engine get preferentially large charge mass fractions, or hold higher cylinder temperatures, then those cylinders will consistently fire hotter and at higher pressures than the other cylinders in the engine. In a Diesel engine, these balance trends can be more pronounced because of the more severe combustion conditions. While, to a certain extent,

the cylinder balancing problem can be accommodated by ‘tuning’ the engine using fuel injection or spark ignition timing, these options are not clear for a HCCI engine.

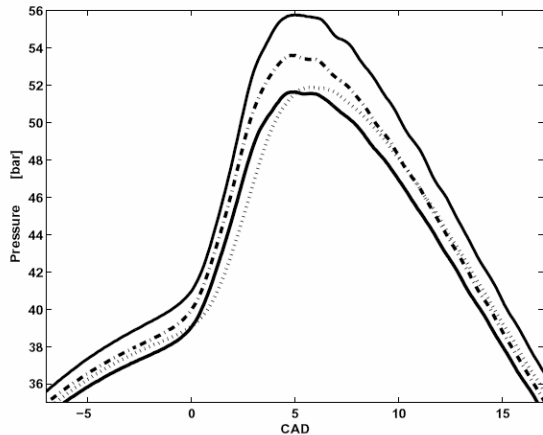


Figure A2: A typical HCCI pressure trace in the TDI engine. The cylinder pressures were intentionally not labeled to emphasize the unbalance. Notice the difference in cylinder compression ratio, pressure, and start of combustion between the four cylinders.

A.4 Causes of Cylinder Imbalance

There are many possible reasons for an engine imbalance. Some explanations are:

- i. A charge distribution problem.
- ii. A temperature distribution problem.
- iii. Different compression ratios in each cylinder.

A charge maldistribution means that the cylinders are combusting different masses of fuel and air every cycle. The disparity in mass is, in turn, attributable to a maldistribution in the intake manifold or to a difference in cylinder compression ratio (cylinder top-land volume). A temperature maldistribution means that either the cylinders in the engine, or the fuel and air coming into the engine, are at different temperatures. The cylinder temperature maldistribution explanation is explored in chapter 5 of this thesis. There is some evidence to support the compression ratio maldistribution theory. In figure A3, notice the difference in compression ratio between the cylinders. At the leftmost edge of the Figure, all cylinder lines should trace one another (have the same pressure value versus CAD). The fact that there is a pressure difference is evidence of a compression ratio difference between the cylinders.

The effect of compression ratio can be seen more clearly in the motoring trace of Figure A3. Notice in Figure A3, that a slight compression ratio difference is evident, with cylinder 4 having the highest cylinder pressure, and cylinder 2 having the lowest cylinder pressure. Because there is no fuel in the cylinders of Figure A3, the cylinder pressure is mostly a function of compression ratio difference. When fuel is added (Figure A3), however, other factors, such as temperature and fuel disproportions, can play a larger part in the cylinder imbalance. Notice that the balance trend is not the same in Figure 4.3 as it is in Figure A3: Cylinder 1 has the lowest pressure in Figure A4, as opposed to Cylinder 2 in Figure A3.

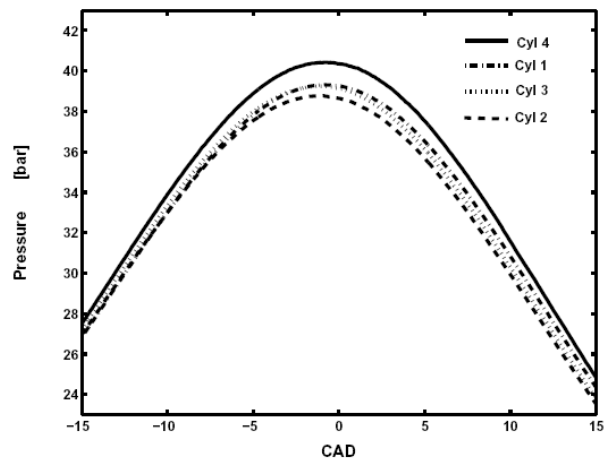


Figure A3: HCCI motoring trace taken from VW TDI engine. Notice the compression ratio difference between cylinders: 4-1-3-2 (highest - lowest)

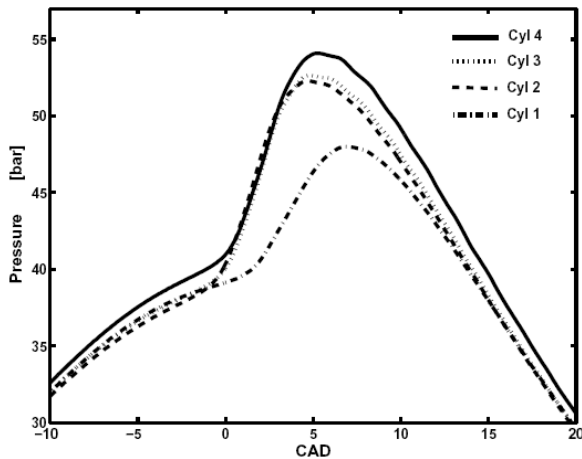


Figure A4: HCCI Firing trace taken from VW TDI engine. Comparing this trace to Figure A3 helps to understand the nature of the cylinder unbalance in the engine. Notice the compression ratio difference between cylinders, (4-3-2-1) which is different from the motoring trace. Also notice the magnitude of the peak pressure differences.

The result of an imbalanced engine is premature wear to the high-load cylinders, and corresponding early failure of those cylinders (and of the engine). In a long-life application, such as power generation, engine fatigue is a major concern. The impetus to correct an imbalanced engine is clear. While the overall goal of this investigation was to explore different methods of control for a HCCI engine, one of the key tasks that the control would purport to accomplish is the balancing of the cylinders.

One technique used to operate HCCI in this investigation was that of intake pre-heating. An 18kW charge air heater was used to boost the intake temperature of the air to levels acceptable for compression-ignited combustion at low equivalence ratios. However, the SOC (calculated according to the equation 2.1) between cylinders remained different at all temperatures, meaning the balancing problem persisted. The same phenomenon was seen with the cylinder peak pressures: despite changing the operating conditions of the engine, the balancing problem remained. Additional methods of control were needed to achieve cylinder balancing.

A.5 Individual Cylinder Intake Preheating

Individual air heaters were placed ahead of the engine block intake ports to individually vary the temperature of the inhaled fuel-in-air inside each cylinder. The heater assembly is shown in Figure 2.3, and described in section 2.3. Four independent voltage controllers were used to supply power to

the intake air heaters. Plotted in Figure A5 and Figure A6 are the variation (standard deviation) of the start of combustion and the peak pressure in the VW TDI engine. The standard deviation is calculated according to equation A1:

$$\sigma = \sqrt{\frac{\sum(x - \mu)^2}{N}}$$

where x can be SOC or pressure for a particular cylinder, μ is the mean SOC or mean pressure for all cylinders, and $N = 4$ is the number of cylinders in the engine. Standard deviation is an indication of the degree of separation between the respective cylinder SOC (pressure) values and the mean SOC (pressure) value - a quantification of the data spread.

The plots of pressure and SOC standard deviation demonstrate successful control of the engine using individual intake air heaters. However, the response time from the heaters was observed to be slow. The thermal inertia of the tube-shaped heaters is thought to have impeded the rapid transition in heater (and intake air) temperature due to a relatively low surface area-to-volume ratio. The response time could be improved with a wire mesh type heater that has more surface area.

A.6 Individual Cylinder Intake Preheating Conclusion

The individual cylinder intake heaters are an effective means at reducing the variation between the cylinders. For both the SOC (Figure A5) and the pressure (Figure A6), the standard deviation is greatly reduced with the addition of intake heating. The peak pressure standard deviation is reduced by up to 88%, from 3.3 to 0.38 bar, and the

SOC standard deviation was reduced by up to 90%, from 1 to 0.1 CAD. Delay time observed in the response time of the heaters is attributable to the thermal inertia of heaters, and may be improved by replacing the bulk tube heaters with wire (more surface area would improve heat transfer).

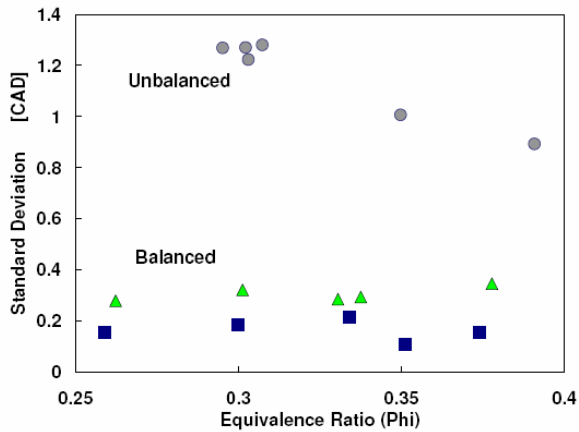


Figure A5: SOC variation with cylinder intake heater balancing. Triangles (80W on cylinder 1) and squares (100W on cyl1 and 20W on cyl2) are balanced cylinders, and circles are unbalanced cylinders. The reduction in standard deviation of SOC with addition of intake heat demonstrates the viability as a control technique.

cylinders, we can conclude that the temperatures between the cylinders are relatively uniform. However, when the SOC between the cylinders is balanced, the peak pressures in the engine remain significantly different (Figure A5 and Figure A6), suggesting that some factor other than the intake temperature is contributing to the cylinder imbalance.

The increase in variation of SOC compared to a decrease in peak pressure variation is surprising, and suggests that additional methods of control are needed for the HCCI engine. The pressure variations are manifestations of a difference in charge mass, cylinder equivalence ratio, or compression ratio; or some combination of the three. Therefore, although individual cylinder intake preheating can help to balance the intake temperature of the engine, it cannot serve as a standalone solution

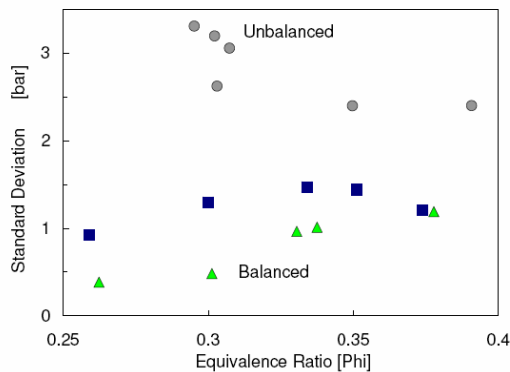


Figure A6: Peak pressure variation with cylinder intake heater balancing. Triangles (80W on cyl1) and squares (100W on cyl1 and 20W on cyl2) are balanced cylinders, and circles are unbalanced cylinders. Notice the decrease in standard deviation of pressure with the addition of intake heating, demonstrating the success of pressure cylinder balancing.

While the SOC may be at the lowest standard deviation condition, the peak pressure variation between cylinders is actually increased (relative to the other ‘balanced’ condition). Notice in Figure 4.4 that with intake heaters on cylinder 1 and 2, the SOC variation is less over the range of equivalence ratios than by just heating cylinder 1. In Figure 4.5, however, the standard deviation of peak pressure actually increases with the heating of cylinder 1 and 2 (versus cylinder 1 only). The lack of correlation between the peak pressure and the SOC implies that more than one factor is unbalancing the engine. For instance, if the SOC in the engine is uniform across all